Neuro-Oncology

20(7), 994–1002, 2018 | doi:10.1093/neuonc/nox227 | Advance Access date 13 December 2017

Cerebral blood flow changes after radiation therapy identifies pseudoprogression in diffuse intrinsic pontine gliomas

Raphael Calmon, Stephanie Puget, Pascale Varlet, Volodia Dangouloff-Ros, Thomas Blauwblomme, Kevin Beccaria, David Grevent, Christian Sainte-Rose, David Castel, Marie-Anne Debily, Christelle Dufour, Stéphanie Bolle, Frederic Dhermain, Ana Saitovitch, Monica Zilbovicius, Francis Brunelle, Jacques Grill,† and Nathalie Boddaert†

Hôpital Necker Enfants Malades, Pediatric Radiology Department, Paris, France (R.C., V.D-R., D.G., F.B., N.B.); Imagine: Institut de Maladies Génétiques, Paris, France (R.C., V.D-R., D.G., A.S., F.B., N.B.); INSERM, Paris, France (R.C., P.V., V.D-R., D.G., A.S., M.Z., F.B., N.B.); Université Paris Descartes, ComUE Sorbonne Paris Cité, Paris, France (R.C., V.D-R., D.G., F.B., N.B.); Hôpital Necker Enfants Malades, Pediatric Neurosurgery Department, Paris, France (S.P., T.B., K.B., C.S-R.); Centre Hospitalier Sainte-Anne, Laboratoire de Neuropathologie, Paris, France (P.V.); Centre National de la Recherche Scientifique, Unité Mixte de Recherche 8203 et Universite Paris Saclay, Villejuif, France (D.C., M-A.D., J.G.); Université Evry Val-d'Essonne, Département de Biologie, Evry, France (M-A.D.); Gustave Roussy, Département de Cancerologie de l'Enfant et de l'Adolescent, Villejuif, France (C.D., F.D., J.G.); Gustave Roussy, Département de Radiothérapie, Villejuif, France (F.D., S.B.)

Corresponding Author: Raphael Calmon, Service de Radiologie Pédiatrique, Hôpital Necker Enfants Malades. 149, rue de Sèvres, 75015 – Paris, France (rcalmon@gmail.com).

†Both Dr Boddaert and Dr Grill have contributed equally as senior authors.

Abstract

Background. The interval between progression and death in diffuse intrinsic pontine glioma (DIPG) is usually <6 months. However, reports of longer patient survival following radiotherapy, in the presence of radiological signs of progression, suggest that these cases may be comparable to pseudoprogression observed in adult glioblastoma. Our aim was to identify such cases and compare their multimodal MRI features with those of patients who did not present the same evolution.

Methods. Multimodal MRIs of 43 children treated for DIPG were retrospectively selected at 4 timepoints: baseline, after radiotherapy, during true progression, and at the last visit. The patients were divided into 2 groups depending on whether they presented conventional MRI changes that mimicked progression. The apparent diffusion coefficient, arterial spin labeling cerebral blood flow (ASL-CBF), and dynamic susceptibility contrast perfusion relative cerebral blood volume (DSCrCBV) and flow (DSCrCBF) values were recorded for each tumor voxel, avoiding necrotic areas.

Results. After radiotherapy, 19 patients (44%) showed radiological signs that mimicked progression: 16 survived >6 months following so-called pseudoprogression, with a median of 8.9 months and a maximum of 35.6 months. All 43 patients exhibited increased blood volume and flow after radiotherapy, but the 90th percentile of those with signs of pseudoprogression had a greater increase of ASL-CBF ($P < 0.001$). Survival between the 2 groups did not differ significantly. During true progression, DSCrCBF and DSCrCBV values increased only in patients who had not experienced pseudoprogression.

Conclusions. Pseudoprogression is a frequent phenomenon in DIPG patients. This condition needs to be recognized before considering treatment discontinuation. In this study, the larger increase of the ASL-CBF ratio after radiotherapy accurately distinguished pseudoprogression from true progression.

Key words

ASL-perfusion | DIPG | MRI | pseudo-progression | radiotherapy

Importance of the study

Misdiagnosis of postradiotherapy changes that mimic tumor progression as progressive disease should be avoided to prevent inappropriate changes in patient care or errors when assessing treatment efficacy in clinical trials. We recorded longitudinal multimodal MRI data of the response of DIPG to treatment with emphasis on previously reported radiotherapy-induced changes that mimic tumor progression.[1] Patients exhibiting signs of pseudoprogression had higher lesion blood flow, as measured by arterial spin labeling sequences that could be used to identify these cases. In addition, tumor perfusion differed during true progression in patients who presented pseudoprogression relative to those who did not, suggesting different pathophysiological processes for response to therapy and tumor progression.

Diffuse midline glioma H3-K27M mutant is a new entity included in the 2016 World Health Organization classification of tumors of the central nervous system, which separates these gliomas, originating in the thalami, brainstem, spine, and sometimes cerebellum in children, from histologically similar adult counterparts according to the presence of a specific histone mutation.[2] Within this entity, the tumors that infiltrate the pons, previously called diffuse intrinsic pontine gliomas (DIPGs), represent a group of pediatric brain tumors with a particularly poor prognosis. No chemotherapy has proven effective, and radiotherapy (RT) is the only recognized treatment that can provide transient disease control. Despite RT, DIPG patients eventually progress and die at a median of 3 to 4 months after progression, with a median overall survival (OS) that varies between 9 and 12 months.[3,4] The molecular biological insights that identified these tumors as single entities also provide a better understanding of their pathophysiology. This could lead to the discovery of better drugs to control this disease, which will require clinical trials to demonstrate their efficacy. Efficacy is usually judged by median OS, since other methods are difficult to standardize. The accuracy and effectiveness of MRI to monitor treatment have yet to be demonstrated.

In 2004, De Wit et al described 3 glioblastoma patients from prospective trials who showed changes in MRI after RT that mimicked disease progression. These changes stabilized or regressed at subsequent examinations.[5] This phenomenon was named pseudoprogression and, at the time, could not be differentiated from true progression. Several studies have since shown that pseudoprogression occurs more frequently within the first 12 weeks after completion of RT in patients treated with temozolomide and those with methylation of the O^6-methylguanine-DNA methyltransferase promoter. Patients experiencing pseudoprogression showed lower cerebral blood volume (CBV) by perfusion imaging, higher apparent diffusion coefficients (ADCs), and lower choline levels by magnetic resonance spectroscopy than those experiencing true progression.[6,7] However, differentiating pseudoprogression from true progression is still challenging and significantly affects patient care and clinical trial evaluation.

A similar phenomenon can be observed in DIPG patients.[1] Some children present radiological changes after RT that mimic tumor progression and at least partially resolve without altering treatment. Their survival after this event is considerably longer than the median 3–4 months after true progression. Our aim was to describe longitudinal changes of multimodal MRI features in an unselected cohort of DIPG patients and compare them with those of patients showing treatment-induced changes that may mimic disease progression.

Materials and Methods

We reviewed the data of all DIPG patients treated in our center from August 2011 to December 2016 whose families authorized the use of clinical and radiological data recorded during treatment for research purposes. Informed consent was obtained according to the institutional review board of the Institut Gustave Roussy. Forty-three patients were included. Stereotactic biopsy was performed on all patients to determine their H3-K27M mutation status. The diagnosis of DIPG for patients for whom the H3-K27M mutation was absent or could not be determined was established by the existence of a high-grade glioma infiltrating the pons with typical clinical and radiological features. All patients received standard RT (54 Gy delivered over 6 weeks). Thirty-seven received either concomitant or adjuvant chemotherapy: erlotinib ($n = 23$), sirolimus ($n = 7$), everolimus ($n = 4$), cilengitide ($n = 2$), and dasatinib ($n = 1$), based on ongoing studies (CILENT-0902, NCT01165333, BIOMEDE, NCT02233049) or previously published protocols,[8,9] and 6 received only RT.

The 43 patients were retrospectively divided into 2 groups depending on whether they had exhibited pseudoprogression or not.

Pseudoprogression was defined as the appearance of radiological signs of tumor progression within 3 months following the completion of RT, in the absence of continuously progressive clinical deterioration, with patient survival >6 months after the event. The Response Assessment in Neuro-Oncology (RANO) criteria[10] were used to define radiological signs of tumor progression: either in T2/fluid-attenuated inversion recovery (FLAIR)–weighted images, as an unequivocal increase in lesion volume, or in contrast enhanced T1-weighted images, as the appearance of new enhancing lesions or a >25% increase in volume of the contrast enhancement component.

True progression was defined as the moment when the disease began to progress, eventually leading to patient death. The date of the beginning of true progression was determined retrospectively by combining radiological findings, using the RANO criteria,[10] the patients' clinical status

(improved, stable, worsened), and the date of death provided by the oncology team.

The multimodal MRI data were acquired from August 2011 to May 2015 on a 1.5T scanner (Signa HDxt, GE Medical Systems). From May 2015 to December 2016, the images were acquired on a 3.0T scanner (MR-750, GE Medical Systems). The routine protocol included morphological and advanced sequences, including volumetric T2 and T2 FLAIR-weighted images and pre- and postcontrast T1-weighted images. Advanced imaging included arterial spin labeling (ASL), multi-b-value diffusion-weighted imaging (DWI), and dynamic susceptibility contrast (DSC) perfusion imaging. A standard dose of 0.1 mmol/kg gadoterate meglumine was administered during DSC acquisition. The injection flow rate was adjusted for a bolus injection lasting 3 s, followed by a saline push. MRI data containing considerable artifacts from patient motion or distortion from implantable material (shunt valves, etc.) were excluded. If necessary, young children were sedated using intrarectal pentobarbital, 5 mg per kg body weight.[11] No general anesthesia was used.

MRI data were collected from the local picture archive and communication system. The multimodal MRI data from up to 4 timepoints were chosen: the examination acquired prior to biopsy and treatment (*baseline*), the examination performed the week following the completion of RT (*after RT*), the examination performed to detect the first signs of true progression of the tumor (*true progression*), and the last available examination (*last visit*). Multimodal MRI data were not available for all patients for *true progression* and *last visit* timepoints, either because patient survival was not long enough for a follow-up scan or because the clinical status of the patient did not justify it. Whether the data were included in the "true progression" or "last visit" timepoint depended on the interval between image acquisition and patient death. The data were included in the *last visit* timepoint if the MRI scan was performed within 90 days of patient death or in the *true progression* timepoint if the interval was longer.

All MRI data were transferred to a workstation running Sphere (Olea Medical) software for postprocessing and analysis. The MRI scanner automatically generated cerebral blood flow maps from the ASL data (ASL-CBF).[12] The DSC perfusion data generated were cerebral blood flow and CBV.[13,14] ADC maps were calculated from the multi-b-value diffusion images using a stretched exponential model.[15] An experienced neuroradiologist, blind to the clinical data, drew regions of interest over the areas with a high T2 signal, corresponding to the tumor in each slice, to create a volume of interest (VOI) while carefully avoiding cystic, necrotic, and hemorrhagic areas to ensure that only live, metabolically active tissue was included. The position of the VOIs was confirmed using postcontrast T1-weighted images, which were transferred to the perfusion and diffusion maps. The intensity of each individual voxel inside the VOIs was recorded for each map and the 10th, 50th (median), and 90th percentile values of the VOIs computed. A VOI of all available, normally appearing, supratentorial white matter for each perfusion map was created using a semi-automated segmentation tool. The mean value of the VOI was used as a reference to calculate the values of DSC relative cerebral blood flow (DSCrCBF) and volume (DSCrCBV).

The results were analyzed using R Project for Statistical Computing (http://www.r-project.org, last accessed December 20, 2017), with the alpha level set at 5%. The *P*-value resulting from Fisher's exact test was used to compare the histone mutation status and distribution of chemotherapy treatment schemes between the 2 groups. The Wilcoxon rank sum test was used to compare the multimodal quantitative data changes over time or between groups, and the Kaplan–Meier log-rank test to estimate and compare survival.

Results

Pseudoprogression in DIPG Patients After Completion of RT

Between August 2011 and December 2016, there were diagnoses of DIPG in 43 patients in our center. The median age was 6 years (range, 2.2–15.3) and 21 of the patients were male. The median progression-free survival (PFS) was 6.5 months (range, 2.0–29.8) and median OS was 9.9 months (range, 2.9–40.9).

After completion of RT, the clinical status of 29 patients (67.4%) improved, remained unchanged for 10 (23.3%), and worsened for the remaining 4 (9.3%), 2 of whom had no radiological evidence of tumor progression. We observed radiological pseudoprogression in 19 patients: increase of contrast enhancement (n = 17), increase of lesion volume in FLAIR images (n = 13), or both (n = 11). Among these 19 patients, 3 survived for <6 months and were excluded from the study as uncertain cases: 2 died 4.6 and 4.4 months after completing RT and were radiologically stable for 2.1 and 4.1 months after RT, respectively, and the last died 24 days after the completion of RT, 15 days after the MRI scan.

Group 1 thus consisted of the remaining 16 patients: median age 5.8 years (range, 2.2–14.4), 8 males. The clinical status improved for 11 patients after RT, remained unchanged for 4, and worsened for 1. They had a median survival of 8.9 months (range, 6.0–35.6) after the initial signs that mimicked progression and subsequently presented signs of progressive disease at a median of 5.9 months (range, 2.1–24.4) later. The median survival after this second event of radiological progression was 4.6 months (range, 0.5–19.2).

Group 2 (control group) included 24 DIPG patients who did not exhibit signs of radiological progression soon after the completion of RT. Their median age was 6.0 years (range, 3.5–15.3) and 12 were male. The clinical status of 17 patients improved after RT, remained unchanged for 5, and worsened for 2. They survived a median of 10.9 months (range, 2.0–32.6) after treatment.

The median PFS was shorter in group 2 (5.0 mo) than in group 1 patients (8.1 mo), but the difference did not reach statistical significance (P = 0.063) when comparing the Kaplan–Meier curves (Fig. 1A). The OS was not significantly different between the 2 groups (Fig. 1B).

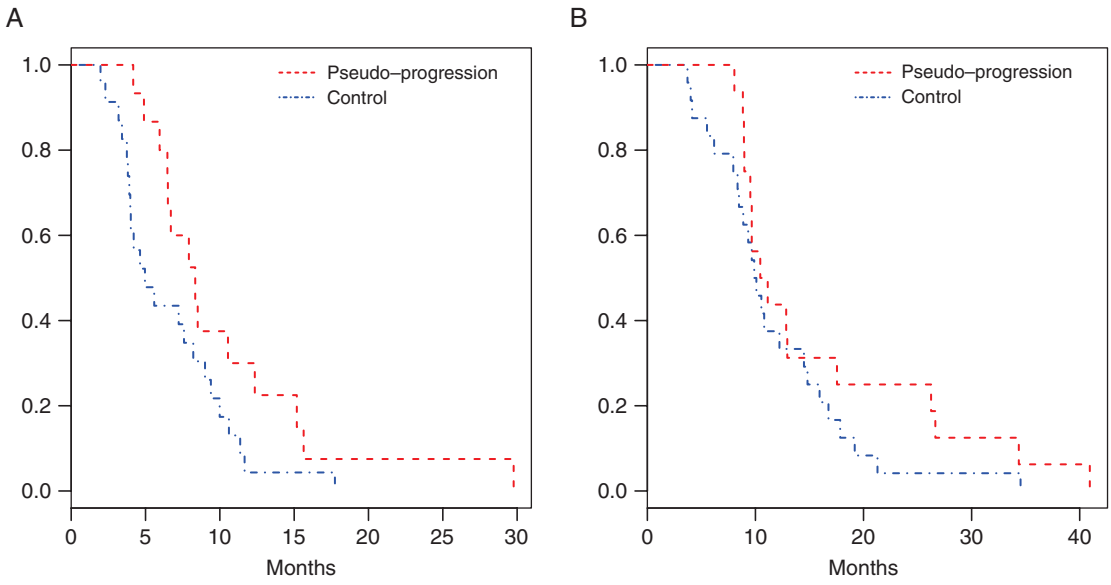

Fig. 1 Kaplan–Meier survival curves of the 2 groups: pseudoprogression (in red), controls (in blue). (A) Progression-free survival. (B) Overall survival.

The histone mutation status was not significantly different between patients from the 2 groups (P = 0.887). Group 1 included 10 H3.3-K27M patients, 4 H3.1-K27M, and 1 H3-wildtype. Group 2 included 12 H3.3-K27M patients, 6 H3.1-K27M, and 3 H3-wildtype. The H3-K27M mutation status could not be determined for 4 patients.

Pseudoprogression occurred in 12 of 27 patients concomitantly treated with radiosensitizers and in 4 of 13 not treated with radiosensitizers (P = 0.503). The distribution of the chemotherapy treatment schemes was not significantly different between the 2 groups (P = 0.601). In group 1, 10 patients were treated with erlotinib, 2 with sirolimus, 1 with everolimus, 1 with dasatinib, and 2 with RT only. In group 2, 10 patients were treated with erlotinib, 5 with sirolimus, 3 with everolimus, 2 with cilengitide, and 4 with RT only.

Longitudinal Radiological Follow-up

Data from the 4 distinct timepoints (baseline, after RT, true progression, last visit) are summarized in Table 1. It contains the median ADC of the 10th and 50th percentiles of all patients and the 50th and 90th percentile ASL-CBF, DSCrCBF, and DSCrCBV values at each timepoint. The same median values were recorded for group 1 and group 2 patients separately. Fig. 2 shows examples of pseudoprogression, illustrated by conventional MRI and multimodal maps.

All Patients

ADC values were elevated at baseline for all patients, decreased after RT, and remained significantly lower than baseline during progression and at the last visit. ASL-CBF values increased significantly (P < 0.001) after RT. They were lower at the true progression (P = 0.001) and last visit (P = 0.001) timepoints than after RT, and not significantly different from baseline values. DSCrCBF (P = 0.001) and DSCrCBV (P < 0.001) values were higher after RT than baseline and lower than after RT at the true progression timepoint (P < 0.001 for both DSCrCBF and DSCrCBV). These values were not significantly different at the last visit timepoint from those of any other timepoint.

Pseudoprogression (Group 1 Patients with Signs of Pseudoprogression After RT)

In group 1 patients, the high ADC values at baseline decreased after RT (P = 0.009) and remained lower than those at baseline at the true progression (P = 0.024) and last visit timepoints (P = 0.012), but were not significantly different from those observed after RT (Fig. 3A in red). The ASL-CBF values after RT were higher than those at baseline (P < 0.001). However, they were lower than those after RT at the true progression (P < 0001) and last visit timepoints (P = 0.002), and were not significantly different from those at baseline (Fig. 3B in red). The DSCrCBF and DSCrCBV values also increased following RT (P = 0.035 and P = 0.21, respectively). They were lower than after RT at the true progression and last visit timepoints and were not significantly different from those at baseline (Fig. 3C and 3D in red).

Control Group (Group 2 Patients with No Signs of Pseudoprogression After RT)

In group 2 patients, the high ADC values at baseline decreased after RT (P = 0.001) and remained lower than

Table 1 Summary of multimodal MRI data for the 4 timepoints

		Baseline		After RT		True Progression		Last Visit	
		Median	IQR	Median	IQR	Median	IQR	Median	IQR
All Patients	ADC p50	2.043	0.935	1.205*	0.412	1.304*	0.284	1.152*	0.222
	ADC p10	1.297	0.510	0.828*	0.241	0.913*	0.190	0.822*	0.274
	ASL-CBF p50	31.00	4.000	52.00*	26.25	33.00†	8.000	33.50†	14.00
	ASL-CBF p90	43.00	6.500	71.50*	40.00	53.00†	10.00	52.00†	16.00
	DSCrCBF p50	1.349	0.877	2.152*	0.972	1.662†	0.512	1.933	1.512
	DSCrCBF p90	2.890	1.656	4.071*	1.623	3.484†	0.809	4.092	1.923
	DSCrCBV p50	1.427	0.546	2.127*	0.738	1.634†	0.575	1.929	1.041
	DSCrCBV p90	2.930	1.147	4.000*	1.527	3.159†	0.801	3.932	2.112
Pseudoprogression Patients	ADC p50	1.842	0.602	1.373*	0.407	1.359*	0.382	1.232*	0.245
	ADC p10	1.251	0.504	0.914*	0.270	0.913*	0.166	0.897*	0.177
	ASL-CBF p50	31.00	2.000	57.00*	28.00	32.00†‡	2.249	32.50†	14.75
	ASL-CBF p90	43.00	6.502	93.00*‡	40.40	46.70†‡	5.000	51.00†	18.48
	DSCrCBF p50	1.369	0.386	2.299*	1.263	1.473†	0.528	1.473†	0.960
	DSCrCBF p90	2.890	1.902	3.988	1.810	3.571	0.503	3.516	1.425
	DSCrCBV p50	1.495	0.503	2.127	0.890	1.605†	0.851	1.573†	0.949
	DSCrCBV p90	2.948	1.172	4.384*	2.015	3.393†	0.805	3.393	1.080
Control Patients	ADC p50	1.604	1.005	1.155*	0.261	1.245*	0.145	1.061*§	0.196
	ADC p10	1.159	0.500	0.811*	0.103	0.916*	0.174	0.760*	0.237
	ASL-CBF p50	31.00	4.500	43.00*	20.00	39.00*‡	7.000	37.00	13.00
	ASL-CBF p90	43.50	5.501	61.00*‡	20.00	56.00*‡	5.001	57.00*	10.00
	DSCrCBF p50	1.139	0.743	2.129*	0.673	1.716†	0.524	2.957*§	1.204
	DSCrCBF p90	2.704	1.445	4.071*	1.271	2.896†	0.660	4.332*§	1.162
	DSCrCBV p50	1.269	0.601	1.972*	0.622	1.663†	0.521	2.563*§	0.897
	DSCrCBV p90	2.979	1.106	3.932*	1.015	3.027†	0.745	4.802*§	1.203

Abbreviations: IQR, interquartile range; ADC, apparent diffusion coefficient (in µm2/ms); ASL-CBF, arterial spin labeling estimated blood flow (in mL/100 g of tissue per minute); DSCrCBF, relative blood flow and DSCrCBV, relative blood volume (both estimated by DSC perfusion); p10, p50, and p90 correspond to the 10th, 50th, and 90th percentile values; * value significantly different from baseline; † value significantly different from after RT; § value significantly different from "progression"; and ‡ significant difference between group 1 and 2 values.

those at baseline at the true progression ($P = 0.004$) and last visit timepoints ($P < 0.001$), but were not significantly different from those observed after RT (Fig. 3A in blue). The ASL-CBF values after RT were higher than those at baseline ($P = 0.001$), but to a lesser extent than those for group 1. During progression, they were not significantly different from those after RT and were significantly higher than those at baseline ($P = 0.043$) (Fig. 3B in blue). The DSCrCBF and DSCrCBV values also increased following RT, increasing transiently ($P = 0.002$ and $P = 0.001$, respectively). Patients with no signs of pseudoprogression were the only ones who showed a second increase in perfusion at the last visit timepoint for both DSCrCBF ($P = 0.011$) and DSCrCBV ($P = 0.002$) (Fig. 3C and 3D in blue).

Differences Between DIPG Patients Who Present with Pseudoprogression and Those Who Do Not

The 2 groups showed no significant differences by multimodal MRI at baseline. The first signs of pseudoprogression were apparent for the MRI scans acquired after the completion of RT at a median interval of 64 days from the time of diagnosis. The after RT scan of control patients (group 2) was performed at a median interval of 60 days after diagnosis. There was no significant difference between the steroid dose administered to the patients in group 1 (median 0.7, range 0.0–2.0 mg/kg) and those in group 2 (median 0.6, range 0.0–2.0 mg/kg) at the time of the MRI scan performed following the completion of RT ($P = 0.705$). The volume of necrosis increased for 12 patients in group 1 and remained stable for the 4 others, whereas it decreased for 2 patients, remained stable for 16, and increased in only 6 from group 2 ($P = 0.005$). Group 1 patients showed slightly higher ADC values, but the difference was not significant. The 90th percentile ASL-CBF values were significantly higher for group 1 patients than for those of group 2 (median 93 vs 61 mL/min per 100 g tissue), $P = 0.022$ (Fig. 4A). The ratio of the increase of the 90th percentile ASL-CBF values from baseline to after RT values was also significantly higher in group 1 patients than those of group 2, $P < 0.001$ (Fig. 4B).

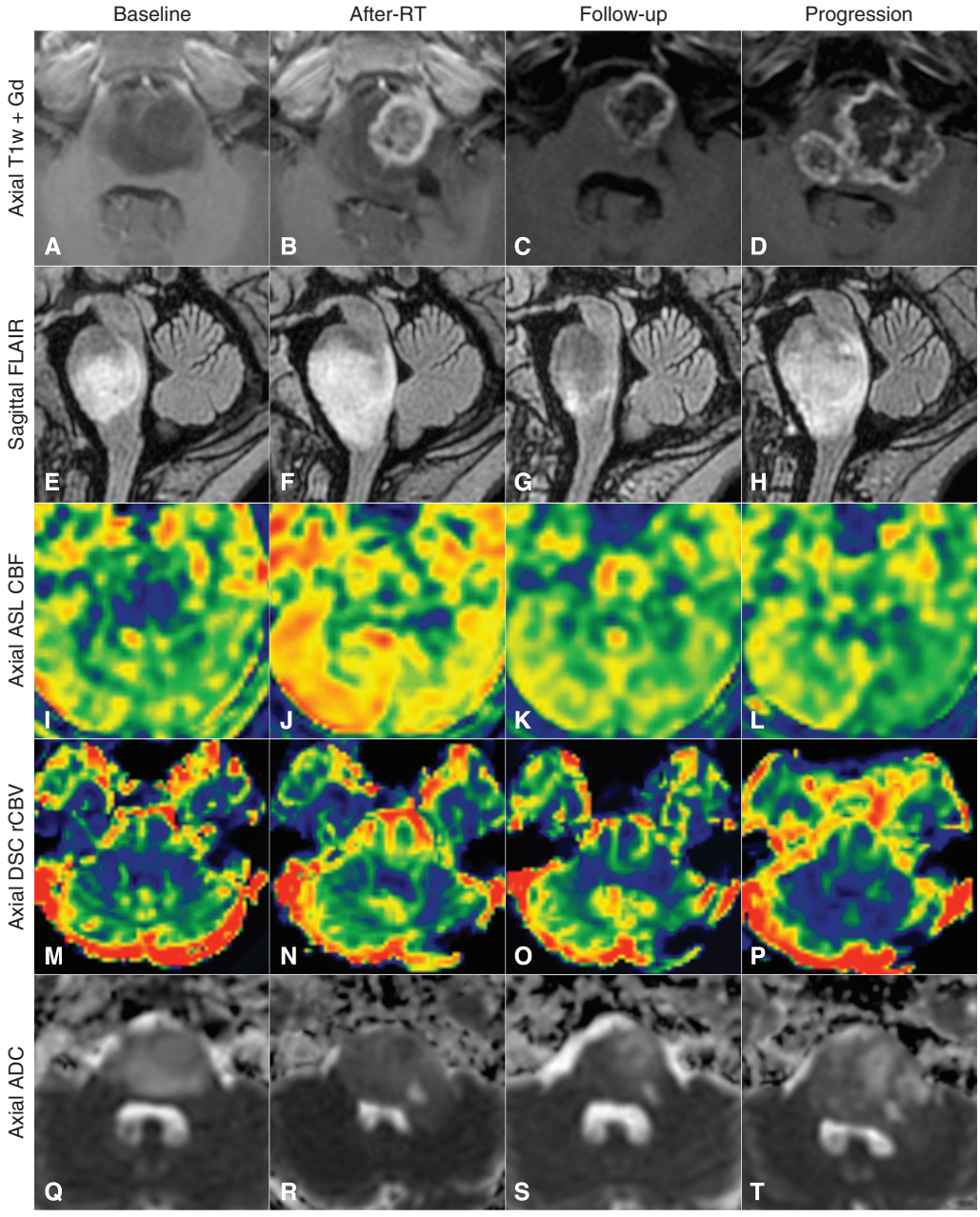

Fig. 2 Longitudinal follow-up of an example case of pseudoprogression with 4 timepoints: at baseline, the week following the end of RT (after RT), at a follow-up examination 3 months after the end of RT, and finally at true progression 9 months after RT. (A–D) Axial T1-weighted images after contrast injection. (E–H) Sagittal T2 FLAIR images, (I–L) axial ASL-CBF, M-P, axial DSCrCBV, Q-T, axial ADC. Note the increase in contrast enhancement and volume of T2 FLAIR abnormalities after RT, associated with increased blood flow and decreased apparent diffusion. These changes reverted spontaneously by a follow-up examination 3 months later.

This ratio (after RT value divided by the baseline value) was the best marker to discriminate between the 2 groups. The use of a threshold of 1.92 (92% increase) correctly differentiated pseudoprogression from control patients with 89% specificity and 100% sensitivity, with an area under the curve of 0.98 (95% CI: 0.93–1; Fig. 4C). The 50th and 90th percentile ASL values during true progression were lower in group 1 than in group 2 ($P = 0.027$ and $P = 0.002$, respectively), as were the 50th percentile DSCrCBF and DSCrCBV values at the last visit timepoint ($P = 0.009$ for both).

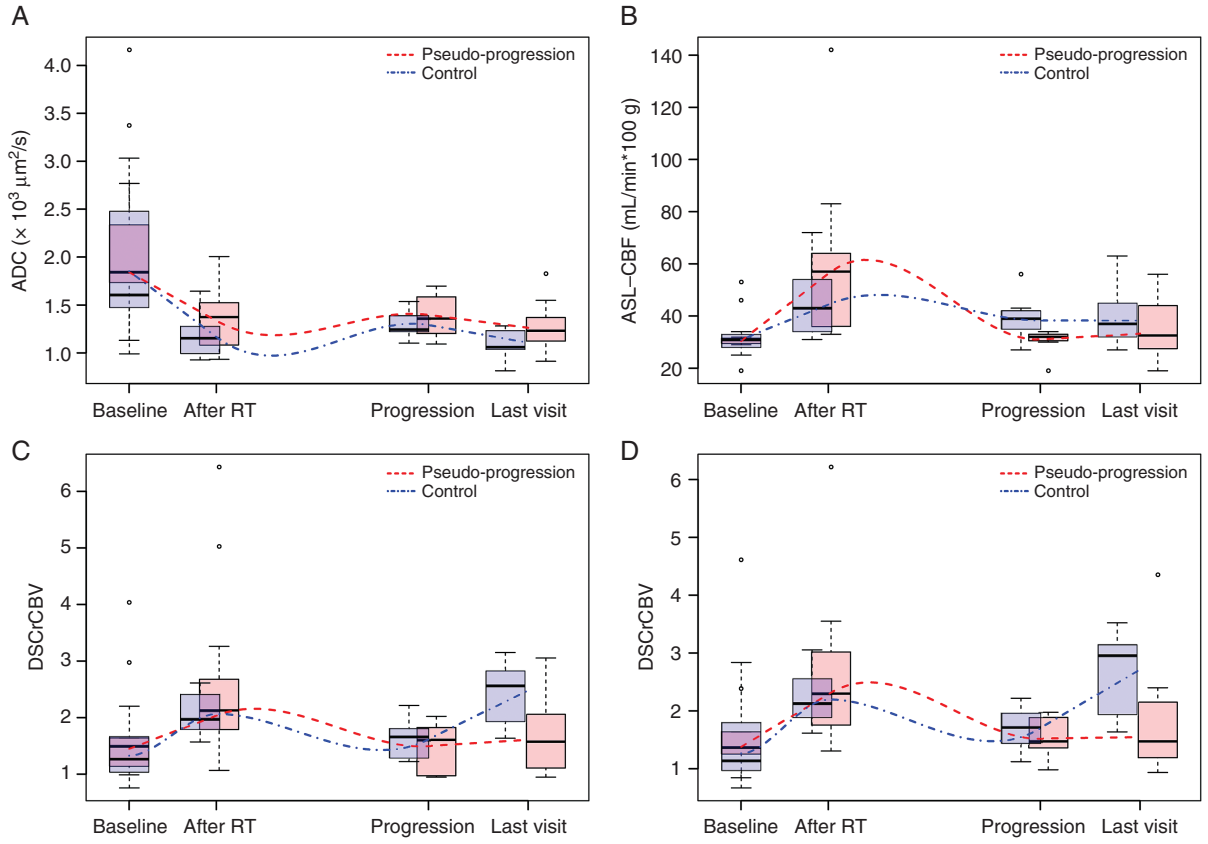

Fig. 3 Boxplot with whiskers representing the distribution of (A) ADC, (B) ASL-CBF, (C) DSCrCBV, and (D) DSCrCBF median values at baseline, after RT, during true progression, and at the last visit for all patients that showed pseudoprogression (in red) and those in the control group (in blue). Lines representing the underlying trend for each group were calculated by local nonparametric regression. Units: ADC in 10^3 µm²/s, ASL-CBF in mL/min per 100 g tissue.

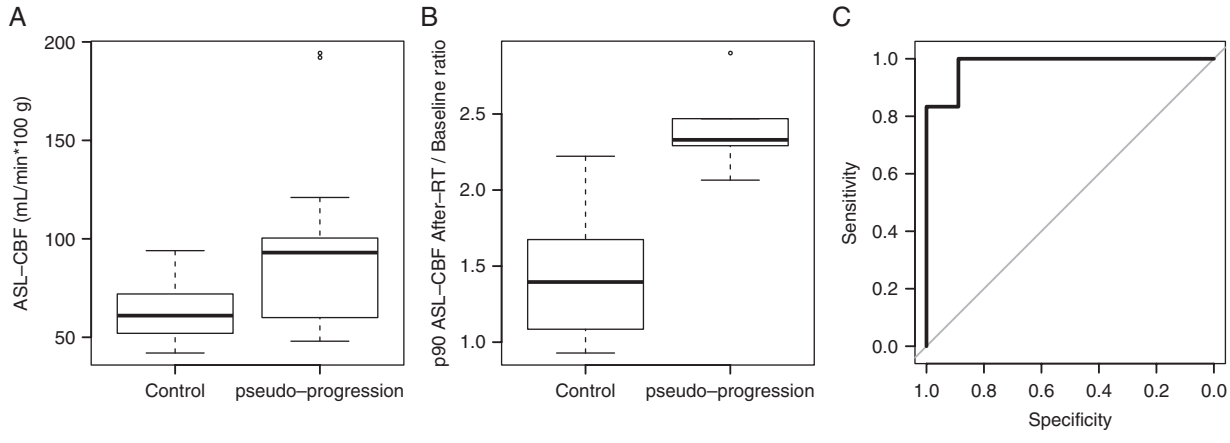

Fig. 4 (A) Boxplot with whiskers representing the distribution of the 90th percentile ASL-CBF after RT values from control and pseudoprogression groups, in mL/min per 100 g tissue. (B) Boxplot with whiskers representing the distribution of after RT/baseline ratios of 90th percentile ASL-CBF values from control and pseudoprogression groups. (C) Receiver operating characteristic curve for identifying pseudoprogression using the after RT/baseline ratio of 90th percentile ASL-CBF values: area under the curve (AUC) = 0.98, best threshold = 1.92, specificity = 89%, sensitivity = 100%.

Discussion

Most current oncology clinical trials include radiological evidence of tumor volume increase as a criterion of disease progression. Transient post-radiation changes that mimic progression, misdiagnosed as progressive disease, can cause errors when assessing treatment efficacy. The RANO working group published an update to the response assessment criteria for adult high-grade gliomas in 2010 to account for this possibility.[10] The RANO group suggests that signs of lesion progression within the irradiation zone must be confirmed either by pathology or a subsequent exam at least 4 weeks later if it occurs during the 12 weeks following RT, because of the higher incidence of pseudoprogression during this period. Histological confirmation of disease progression in DIPG patients is not feasible and the morphological changes usually occur within the radiation field. Failure to recognize pseudoprogression in DIPG could lead to an underestimation of treatment efficacy and end the investigation of new potentially effective drugs. However, to consider every case with signs of lesion progression following RT as pseudoprogression may delay treatment changes in patients with progressive disease who have short survival. A working group to propose specific criteria to address these issues, as well as others in pediatric neuro-oncology, has been established. However, its recommendations have yet to be published.[16]

In the present study, 19 of 43 children exhibited morphological changes after completion of RT that could be classified as progression, according to the RANO criteria. Three died early or could not be analyzed properly. The survival of each of the remaining 16 children was much longer than the median 4-month survival after progression reported in the literature.[4] All but one patient then presented de novo signs of progression. Survival after this second event was as expected (median 4.6 mo), suggesting that this time, MRI indicated true tumor progression.

In addition to the median value (50th percentile), we measured the 10th and 90th percentiles to emulate current clinical practice, in which a region of interest is normally drawn over the "hot spot" of the lesion. The higher 90th percentile ASL-CBF ratio of children exhibiting pseudoprogression after RT could discriminate between the 2 groups. The threshold of 1.92 may be useful in clinical practice when DIPGs show signs of progression after the completion of RT, but will require the use of multimodal MRI techniques at these timepoints. The differences in ASL and DSC perfusion between group 1 and group 2 patients found at the true progression and last visit timepoints suggest that different pathophysiological processes may be involved in disease progression and pseudoprogression in response to RT. The process in patients that showed pseudoprogression is signaled by marked increase of ASL-CBF, DSCrCBF, and DSCrCBV following RT, which then decrease and remain low until the end of the patient's life. The process in patients who did not show pseudoprogression after RT is signaled by ASL-CBF, DSCrCBF, and DSCrCBV that do not increase as much, with an ASL-CBF that remains elevated and DSCrCBF and DSCrCBV that increase toward the end of the patient's life.

Radiation causes acute brain tissue injury by 3 mechanisms: directly by oxidative stress, indirectly by cytokine-mediated inflammation, or directly by damaging and killing endothelial cells that may have an anti-angiogenic effect.[17–20] After RT, the DIPG patients in this study showed a decreased ADC, indicating less tissue edema and more blood flow than at baseline, suggesting remodeling that results in a more efficient vascular bed. These observations are consistent with previous reports that described DIPGs as tumors that show a transitory increase in blood flow and blood volume during and following RT,[21] for which the elevated ADC values at baseline decrease after RT.[22,23] These changes observed in DIPGs in response to treatment are similar to those observed in tumors treated with anti-angiogenic agents, such as anti–vascular endothelial growth factor drugs. In such cases, these drugs are thought to induce "normalization" of the tumor vascular bed. These "normalized" vessels allow increased blood flow and are less permeable, eventually resulting in decreased tissue hydrostatic pressure and edema.[17,24]

One limitation of this study is the limited number of patients inherent to studies of rare diseases. In addition, the patients were submitted to varying treatment regimes, but there was no significant difference in their distribution between the 2 groups.

In conclusion, we have observed radiological signs of progressive disease after completion of RT without truly progressive disease in 40% of DIPG patients. We recommend that morphological changes accompanied by increased lesion blood flow be considered as potential pseudoprogression and that adjuvant treatment not be discontinued. The patients of the 2 groups appear to be affected by 2 different processes of vascular change near the end of their lives that merit further investigation.

Funding

This work was funded by grants from L'Etoile de Martin and the Fondation Lemos awarded to J.G. and D.C.

Conflict of interest statement. Jacques Grill declares grant support for conducting trials with Hoffmann-La Roche, Novartis, and Bristol-Myers Squibb. No other author declares a conflict of interest.

References

1. Chassot A, Canale S, Varlet P, et al. Radiotherapy with concurrent and adjuvant temozolomide in children with newly diagnosed diffuse intrinsic pontine glioma. *J Neurooncol*. 2012;106(2):399–407.
2. Louis DN, Perry A, Reifenberger G, et al. The 2016 World Health Organization classification of tumors of the central nervous system: a summary. *Acta Neuropathol*. 2016;131(6):803–820.
3. Bredlau AL, Korones DN. Diffuse intrinsic pontine gliomas: treatments and controversies. *Adv Cancer Res*. 2014;121:235–259.

4. Van Zanten SEMV, Baugh J, Chaney B, et al. Development of the SIOPE DIPG network, registry and imaging repository: a collaborative effort to optimize research into a rare and lethal disease. *J Neurooncol* 2017;0:1–12.
5. de Wit MC, de Bruin HG, Eijkenboom W, Sillevis Smitt PA, van den Bent MJ. Immediate post-radiotherapy changes in malignant glioma can mimic tumor progression. *Neurology*. 2004;63(3):535–537.
6. Ryken TC, Aygun N, Morris J, et al; AANS/CNS Joint Guidelines Committee. The role of imaging in the management of progressive glioblastoma: a systematic review and evidence-based clinical practice guideline. *J Neurooncol*. 2014;118(3):435–460.
7. Ellingson BM, Chung C, Pope WB, Boxerman JL, Kaufmann TJ. Pseudoprogression, radionecrosis, inflammation or true tumor progression? challenges associated with glioblastoma response assessment in an evolving therapeutic landscape. *J Neurooncol* 2017;77:1–10.
8. Geoerger B, Hargrave D, Thomas F, et al; ITCC (Innovative Therapies for Children with Cancer) European Consortium. Innovative Therapies for Children with Cancer pediatric phase I study of erlotinib in brainstem glioma and relapsing/refractory brain tumors. *Neuro Oncol*. 2011;13(1):109–118.
9. Geoerger B, Kieran MW, Grupp S, et al. Phase II trial of temsirolimus in children with high-grade glioma, neuroblastoma and rhabdomyosarcoma. *Eur J Cancer*. 2012;48(2):253–262.
10. Wen PY, Macdonald DR, Reardon DA, et al. Updated response assessment criteria for high-grade gliomas: response assessment in neuro-oncology working group. *J Clin Oncol*. 2010;28(11):1963–1972.
11. Dangouloff-Ros V, Deroulers C, Foissac F, et al. Arterial spin labeling to predict brain tumor grading in children: correlations between histopathologic vascular density and perfusion MR imaging. *Radiology*. 2016;281(2):553–566.
12. Lehmann P, Monet P, de Marco G, et al. A comparative study of perfusion measurement in brain tumours at 3 Tesla MR: Arterial spin labeling versus dynamic susceptibility contrast-enhanced MRI. *Eur Neurol*. 2010;64(1):21–26.
13. Boutelier T, Kudo K, Pautot F, Sasaki M. Bayesian hemodynamic parameter estimation by bolus tracking perfusion weighted imaging. *IEEE Trans Med Imaging*. 2012;31(7):1381–1395.
14. Harris RJ, Cloughesy TF, Hardy AJ, et al. MRI perfusion measurements calculated using advanced deconvolution techniques predict survival in recurrent glioblastoma treated with bevacizumab. *J Neurooncol*. 2015;122(3):497–505.
15. Kwee TC, Galbán CJ, Tsien C, et al. Comparison of apparent diffusion coefficients and distributed diffusion coefficients in high-grade gliomas. *J Magn Reson Imaging*. 2010;31(3):531–537.
16. Warren KE, Poussaint TY, Vezina G, et al. Challenges with defining response to antitumor agents in pediatric neuro-oncology: a report from the Response Assessment in Pediatric Neuro-Oncology (RAPNO) working group. *Pediatr Blood Cancer*. 2013;60(9):1397–1401.
17. Jain RK. Normalization of tumor vasculature: an emerging concept in antiangiogenic therapy. *Science*. 2005;307(5706):58–62.
18. Tofilon PJ, Fike JR. The radioresponse of the central nervous system: a dynamic process. *Radiat Res*. 2000;153(4):357–370.
19. Kim JH, Jenrow KA, Brown SL. Mechanisms of radiation-induced normal tissue toxicity and implications for future clinical trials. *Radiat Oncol J*. 2014;32(3):103–115.
20. Garcia-Barros M, Paris F, Cordon-Cardo C, et al. Tumor response to radiotherapy regulated by endothelial cell apoptosis. *Science*. 2003;300(5622):1155–1159.
21. Sedlacik J, Winchell A, Kocak M, Loeffler RB, Broniscer A, Hillenbrand CM. MR imaging assessment of tumor perfusion and 3D segmented volume at baseline, during treatment, and at tumor progression in children with newly diagnosed diffuse intrinsic pontine glioma. *AJNR Am J Neuroradiol*. 2013;34(7):1450–1455.
22. Poussaint TY, Kocak M, Vajapeyam S, et al. MRI as a central component of clinical trials analysis in brainstem glioma: a report from the Pediatric Brain Tumor Consortium (PBTC). *Neuro Oncol*. 2011;13(4):417–427.
23. Chen HJ, Panigrahy A, Dhall G, Finlay JL, Nelson MD Jr, Blüml S. Apparent diffusion and fractional anisotropy of diffuse intrinsic brain stem gliomas. *AJNR Am J Neuroradiol*. 2010;31(10):1879–1885.
24. Carmeliet P, Jain RK. Principles and mechanisms of vessel normalization for cancer and other angiogenic diseases. *Nat Rev Drug Discov*. 2011;10(6):417–427.